Very Slow Activity Fluctuations in Monkey Visual Cortex: Implications for Functional Brain Imaging

David A. Leopold, Yusuke Murayama and Nikos K. Logothetis

Max Planck Institut für biologische Kybernetik,
Spemannstraße 38, 72076 Tübingen, Germany

We examined fluctuations in band-limited power (BLP) of local field potential (LFP) signals recorded from multiple electrodes in visual cortex of the monkey during different behavioral states. We asked whether such signals demonstrated coherent fluctuations over time-scales of seconds and minutes, and would thus serve as good candidates for direct comparison with data obtained from functional magnetic resonance imaging (fMRI). We obtained the following results. (i) The BLP of the local field displayed fluctuations at many time-scales, with particularly large amplitude at very low frequencies (<0.1 Hz). (ii) These fluctuations exhibited high coherence between electrode pairs, particularly for BLP signals derived from the gamma (γ) frequency range. (iii) Coherence in the BLP, unlike that in the raw LFP, did not fall off sharply as a function of cortical distance. (iv) The structure and coherence of BLP changes were highly similar under distinctly different behavioral states. These results demonstrate the existence of widespread coherent activity fluctuations in the brain of the awake monkey over very long time-scales. We propose that such signals may make a significant contribution to the high variability observed in the time course of physiological signals, including those measured with functional imaging techniques. The results are discussed in the context of combined fMRI/electrophysiological recordings.

Introduction

Accurate interpretation of neurophysiological signals requires that they be taken in the context of existing activity patterns in the brain. While this tenet is clearly important for the scientist attempting to decipher highly variable neural measurements, it is also of fundamental importance to brain function – the brain must be able to understand its own variability. A number of recent studies have underscored the practical importance of this theoretical consideration for the processing of sensory patterns, demonstrating that the responses of neurons are predetermined by existing brain-states rather than simply by an externally applied stimulus (Arieli *et al.*, 1995, 1996; Azouz and Gray, 1999; Steriade, 2001a). To reliably interact with their environment, brains must somehow disentangle stimulus-related information from that reflecting changes in its internal milieu; and they evidently do so with great success. How this is done remains poorly understood.

While it is clear that this process must draw upon a careful balance between local (intra-area) and global (inter-area) processing, it is gradually becoming apparent that sensory information does not flow unidirectionally through a chain of discrete processing stages. Response latency measurements, for example, suggest that visual stimuli are processed by a highly complex, parallel and recurrent cortical network (Bullier and Nowak, 1995; Schmolesky *et al.*, 1998; Schroeder *et al.*, 1998; Lamme and Roelfsema, 2000). Other studies have argued that the flow of information through this network is inherently multi-directional (Hupe *et al.*, 1998; Lamme *et al.*, 1998). At the same time, the basic role played by the thalamus in mediating interactions within this cortical network – when not ignored – is strongly debated (Ramcharan *et al.*, 2000; Sherman and Guillery, 2000; Steriade, 2000, 2001b). Using traditional neurophysiological techniques to address the brain's global scheme for processing its input is challenging, as it involves the targeted placement of multiple electrodes in diverse brain areas. While such approaches have been used successfully (Nicolelis *et al.*, 1995; von Stein *et al.*, 1997; Kara *et al.*, 2000), the spatial coverage afforded by such methods is inherently limited by the positioning of the electrodes, which is, in turn, constrained by the priors and hypotheses of the investigator. In contrast, a great strength of functional brain imaging, in particular functional magnetic resonance imaging (fMRI), is that it can provide a global view of activity throughout the brain, allowing one to simultaneously monitor the functional changes in distant cortical and subcortical structures. For this reason, as well as its non-invasive nature, it has in the last decade become the dominant tool for studying human brain function (Frackowiak *et al.*, 1997). Recently fMRI has been introduced as a much-needed addition to the repertoire of tools used to study the brain of nonhuman primates (Logothetis *et al.*, 1999).

Unfortunately, the spatial and temporal resolution of the fMRI signal are currently poor compared to neurophysiological methods. Many of its limitations stem from the fact that it measures a surrogate signal rather than neuronal activity directly. Specifically, most contrast mechanisms, such as the popular BOLD (blood oxygen level dependent) technique, are driven by blood flow and volume changes that are secondary to metabolic changes caused by neural activity. Recent studies have demonstrated that while such signals are tightly coupled to neural activity, in particular to the LFP (Logothetis *et al.*, 2001), they are sluggish in their temporal response, often requiring seconds to register a change. Compared with electrophysiological recordings, which register neural events at arbitrarily short time-scales, BOLD imaging is at least three orders of magnitude worse at tracking dynamic aspects of neural activity relevant for cognition and behavior, but see Ogawa *et al.* (Ogawa *et al.*, 2000). Given that the strengths and weaknesses of electrophysiological and fMRI techniques are in some sense complementary, a number of previous human studies have sought to combine the two techniques, with the aim of gaining spatial localization from fMRI and temporal information from electroencephalographic (EEG) measurements (Heinze *et al.*, 1994; Bonmassar *et al.*, 2001). Of particular interest to the current study is the recent emergence of combined techniques in the nonhuman primate, where it is now possible to monitor neural activity at one or more intracranial sites during high resolution fMRI scanning (Logothetis *et al.*, 2001). This combination affords the direct comparison of cortical signals (spiking or local field) with the BOLD fMRI signal and promises new insights into brain function that neither signal alone could provide.

The present study represents a first step toward exploring the possibility that combined electrophysiology and fMRI methods can be used to investigate endogenous activity changes in the brain, including those related to the signal variability mentioned above. The supposition is that a continuously monitored neural signal can serve as a useful reference for functional imaging, allowing one to focus on spontaneous changes in the BOLD signal that are of neural origin. Here we concentrate on one aspect of this newly starting research line: what kinds of electrophysiological activity fluctuations might best be correlated with the time course of individual voxels obtained from functional imaging? Specifically, we seek temporal patterns in the neural signal that occur very slowly and can thus be directly compared with changes in the BOLD signal. Fluctuations in the raw local field voltage itself are an improbable candidate since neurophysiological measurements are generally filtered to eliminate changes on time-scales longer than a second. While it would be possible to minimize such filtering in order to track very slow potential changes (Bauer and Rebert, 1990), we focus instead on changes in the local field power, since previous results found LFP power to be well correlated with BOLD responses to sensory stimuli (Logothetis *et al.*, 2001). We begin by extracting a family of band-limited power (BLP) signals from a single LFP trace and demonstrate that these extracted signals possess large-amplitude fluctuations over very long time-scales (>10 s) during different behavioral states. We then show that these fluctuations are highly coherent between electrodes whose effective cortical separation exceeds even 25 mm. We propose that these very slow, highly coherent fluctuations in neural activity are perfectly suited for measurement with fMRI and are therefore likely to have a large impact on the BOLD signal. We discuss the merits of combined electrophysiological/ fMRI recordings in the context of (i) studying brain networks that contribute to this variability and (ii) removing 'physiological noise' that is unrelated to a fixed stimulus paradigm.

Materials and Methods

Two adult rhesus monkeys, K97 and R97, were used in the experiments, and participated in 21 and two experimental sessions, respectively. During each session, data was recorded while the animal either executed a behavioral task (K97 only, task described below) or sat quietly in a dimly lit room (both animals). Results from the two animals were similar, and are thus considered together. All experiments were performed in compliance with the guidelines of the local authorities (Regierungspraesidium) as well as the European Community (EUVD 86/609/EEC) for the care and use of laboratory animals.

Surgery

Details of the surgical procedures can be found elsewhere (Logothetis *et al.*, 1999; Leopold *et al.*, 2002). Briefly, the animal was implanted under sterile conditions with a custom-made, single piece titanium head holder. In a second surgery, an occipital recording chamber was implanted and a large (23 mm) craniotomy was made, permitting direct access to the brain through the dura mater. A cylindrical chamber constructed of plastic (Tecapeek, GF 30; Ensinger GmbH, Germany) was attached to the skull with ceramic screws. Following surgery, the animal spent 10 days in a recovery chair, which allowed him to stand and move freely, but did not permit touching of the fresh implants. Analgesic (Finadyne, 1.0 mg/kg) was given during the first two days, as well as antibiotic (Veracin Composite, 0.25 ml/kg) for 8 days after the surgery.

Electrophysiology

Intracortical recordings were conducted with the Eckhorn multielectrode array (Eckhorn and Thomas, 1993), permitting the simultaneous monitoring of up to 15 sites (one channel was reserved for synchronization with the computer). Electrodes were $Pt_{90}W_{10}$ wire (diameter = 20 μm) with a glass coating (external diameter = 80 μm), and were guided into the brain each day through the overlying dura mater. The recording chamber was situated over the lunate sulcus (Fig 1*a*), and afforded a large field for data collection. During the recordings, a custom-made adaptor was used to distribute the electrodes against the dura in a 4 × 4 square array, with an inter-electrode spacing of 2.5 mm. Thus, the closest electrode pairs were separated by 2.5 mm, while the farthest (opposite corners) were had a physical separation of 10.6 mm.

Two fundamentally different electrode-positioning strategies were

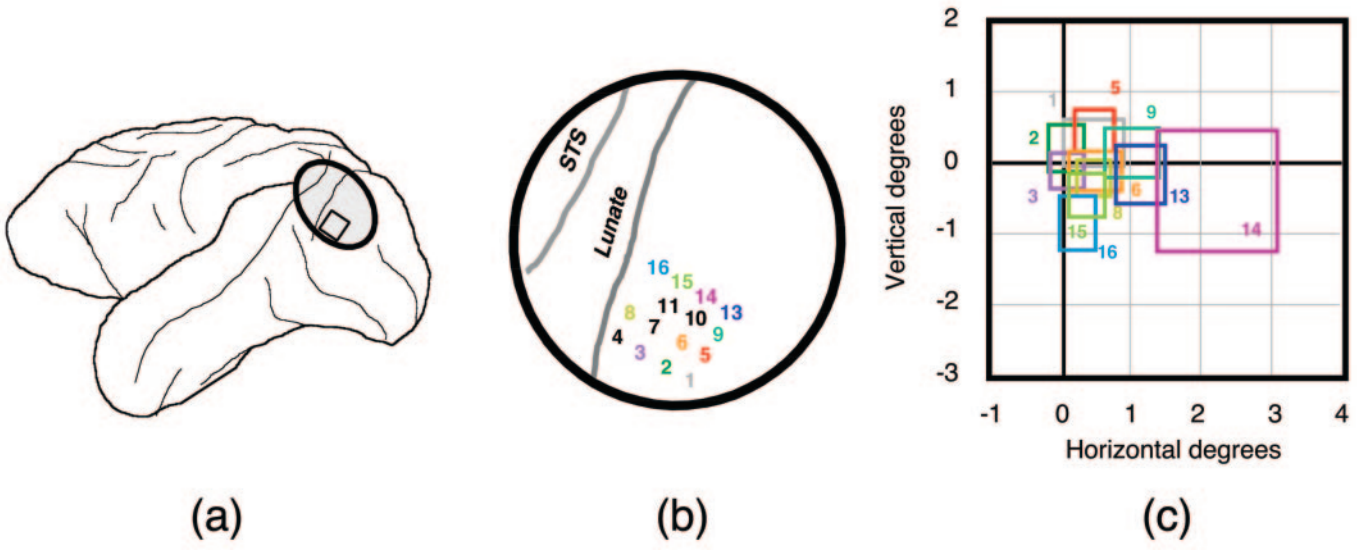

Figure 1. Chamber, recording sites and receptive field positions. (*a*) A 23 mm inner-diameter chamber was placed over the left hemisphere (Horsley–Clark coordinates 7 P, 25 L_{LEFT}, 12 D_{HC}), straddling the lunate and superior temporal sulci. This position allowed easy access to several early visual areas. (*b*) Example of recording sites in this study. Electrodes were spaced in a square array, with an inter-electrode separation of 2.5 mm along the cortical surface. In this example, transdural electrode penetrations were perpendicular to the underlying cortex posterior to the lunate sulcus, in visual areas V1 and V2. In such cases, the inter-electrode separation was a good approximation of effective cortical distance between electrode pairs. In contrast, in some sessions the recording device was placed more anterior, with a subset of electrodes on either side of the lunate sulcus (see Fig. 10). In such cases, the effective cortical distance for electrodes on opposite sides of the sulcus was much larger. For this reason, the analysis in this paper was restricted to the position shown here. (*c*) Receptive field positions for the cortical positions shown in (*b*).

applied in this study. In the first configuration (Fig. 1*b*), the entire electrode array was placed posterior to the lunate sulcus. This positioning ensured that the effective cortical separation between each electrode pair corresponded roughly to their horizontal distance. In the second configuration (Fig. 10), the electrode array straddled the lunate sulcus, with a portion of the electrodes on the prelunate gyrus in area V4. In this setup, the effective cortical distance was significantly larger between those electrodes on opposite sides of the sulcus (>25 mm), even though the horizontal distance between the electrodes was the same. Each day, all electrodes were positioned in the cortex, and receptive field sizes and positions were first carefully mapped (for K97 only), as shown for the example in Fig 1*c*. In general, the recordings were conducted in the superficial layers of cortex, shortly following penetration of the dura.

Behavioral Conditions and Data Collection

Neural activity was monitored with the electrodes in a given position during two distinctly different behavioral conditions. In the rest condition, activity was monitored from the same electrodes in the same positions, but while the monkey had no behavioral requirements. During this period, which typically lasted 30–60 min, the monkey sat alone in a dimly lit room. Eye movements during this condition revealed some periods of normal scanning movements, and others of slow drift, consistent with the animal entering light sleep. The eyes would sometimes close, although we did not have the impression that the monkey entered deep sleep since they would only stay closed for a few seconds or minutes at a time.

In addition, we tested monkey K97 under conditions in which he was actively engaged in a binocular rivalry task (task condition). Task details of this paradigm are provided elsewhere (Leopold and Logothetis, 1996). Briefly, the monkey would acquire and hold fixation for periods lasting between 10 and 20 s, during which time a variety of stimuli were shown. The stimuli were in general effective at driving neurons at the sites we recorded, although they were tailored to perceptual criteria rather than to the preferences of the neurons. The monkey's task was to observe the stimulus and respond to changes in the perceptual dominance of two competing visual patterns. At the end of a successful observation period, the monkey received ~0.5 ml of apple juice as a reward. Neural signals were also recorded during the 3–5 s intertrial interval, during which time the animal rested. Throughout the task, data was collected 'pseudo-continuously', with brief interruptions in recording for a few hundred milliseconds between trials.

During the rest and task conditions, data collection was controlled by an industrial PC (Advantech) running under the QNX operating system (QNX Software Systems, Kanata, Ontario, Canada). The local field data from each channel were amplified by a factor of 8000 and band-pass filtered between 1 Hz (two pole Butterworth filter) and 1 kHz (four pole Butterworth filter) (Alpha Omega Engineering, Nazareth, Israel). The signals were then individually digitized at a rate of 4.5 kHz on a 12-bit analog to digital board (Win30; United Electronic Industries, Watertown, MA) and stored on a PC for further analysis using custom software written in MATLAB (The Mathworks Inc., Natick, MA).

Band Limited Power Calculation

For each LFP signal, the BLP was calculated as follows. For the task condition, LFP data from individual observation periods were concatenated to provide a nearly continuous signal (see above). In the rest condition, data collection was uninterrupted. Each condition therefore yielded continuous signals corresponding to recording periods lasting between 30 (rest) and 90 (task) min.

The LFP signals were resampled to 1 kHz, and then band-pass filtered into seven frequency ranges using a second order, bi-directional, zero-phase Chebyshev type-1 filter. The frequency ranges, as well as their rough mapping onto classically defined electroencephalographic conventions, were the following: δ (1–4 Hz), θ (5–8 Hz), α (9–14 Hz), β (15–30 Hz), γ_L (30–50 Hz), γ_H (50–100 Hz), and γ_{VH} (100–150 Hz). The resulting band-limited signals were full-wave rectified by taking their absolute value. They were then resampled to 20 Hz after low-pass filtering with an eighth order Chebyshev type-1 filter (cutoff = 8 Hz). The most relevant conceptual steps in this processing are illustrated schematically in Figure 4*a*. Note that a particularly important step in the LFP signal processing is the rectification stage, which provides a measure of the time-varying envelope amplitude of each band-pass filtered signal. Once rectified, the signal can contain arbitrarily low frequencies, and is no longer a measure of voltage but rather power (in actuality, the square root of the power). This rectification stage is directly analogous to that used in the demodulation of an AM radio signal, where the temporal structure of the envelope is of interest, rather than the carrier frequency itself. By filtering a given LFP signal according to each of the predefined bandwidths and then rectifying the outcome, we obtain a family of BLP signals, each of which represents the temporal structure of power fluctuations within a given frequency range (e.g. α, β, γ, etc.). From another perspective, a given BLP signal is roughly equivalent to mean of several rows of a spectrogram, or time-frequency plot. Averaging several adjacent rows of a spectrogram together similarly provides a time-varying signal corresponding to the evolving power in a given frequency range.

Coherence Analysis

For both the raw and BLP signals, magnitude squared coherence, $C_{xy}(f)$, was calculated between electrode pairs, according to the formula:

$$C_{xy}(f) = \frac{\left|P_{xy}(f)\right|^2}{P_{xx}(f)P_{yy}(f)}$$

where $P_{xx}(f)$ and $P_{yy}(f)$ are the power spectra of x and y of each individual signal and $P_{xy}(f)$ is their cross spectrum. Time windows were combined using Welch's averaged periodogram method, with the overlap of successive windows for raw and BLP signals of 25 and 95%, respectively. The resulting coherence functions provided a measure of signal covariation, or coupling, as a function of frequency. For the raw signal, the sampling frequency (F_s) was 1.0 kHz, with a typical recording duration of 20–30 min (>10^6 points). Each fast Fourier transform (FFT) was computed with 16 384 (2^{14}) points, providing a spectral resolution of 0.06 Hz. For the BLP signal, where the F_s was 20 Hz, an FFT of length 2048 (2^{11}) was used, resulting in a spectral resolution of 0.01 Hz.

Results

Coupling of Raw LFP Signals

We began by examining the power and coherence characteristics of the raw (unprocessed) local field signals during task and rest conditions. For this first phase of the analysis, these two conditions provided three distinct periods for comparison: (i) activity during active engagement in the visual task, (ii) activity in the inter-trial period of the task condition, where the monkey relaxed for 2–3 s, and (iii) activity during the rest condition, when the monkey sat uninterrupted for 20–40 min. Figure 2*a* depicts the average spectral power of a representative session under these three different states. Each curve represents the mean power spectrum from 15 electrodes at the positions depicted in Figure 1. Note that each of the curves shows its highest power at low frequencies, with a decline in spectral power between 3 and 30 Hz. For the task condition, there is an additional well-defined peak in the γ-range (30–80 Hz) that is absent in the other conditions. The transmission of frequencies <1 Hz was limited by a high-pass hardware filter.

To examine coupling between the signals measured at different electrodes, we computed the coherence functions between all electrode pairs, which is shown in Figure 2*b* for the three conditions. In general, coherence values decreased with increasing frequency between 8 and 100 Hz. For lower frequencies, the pattern was highly dependent on the behavioral state, with the task condition showing a marked absence of coherence (i.e. desynchronization) below 6 Hz compared to the other conditions. In order to evaluate the impact of cortical distance on the LFP coupling, we computed coherence functions for each of the possible inter-electrode distances. Figure 3 demonstrates that the separation between cortical electrodes is a

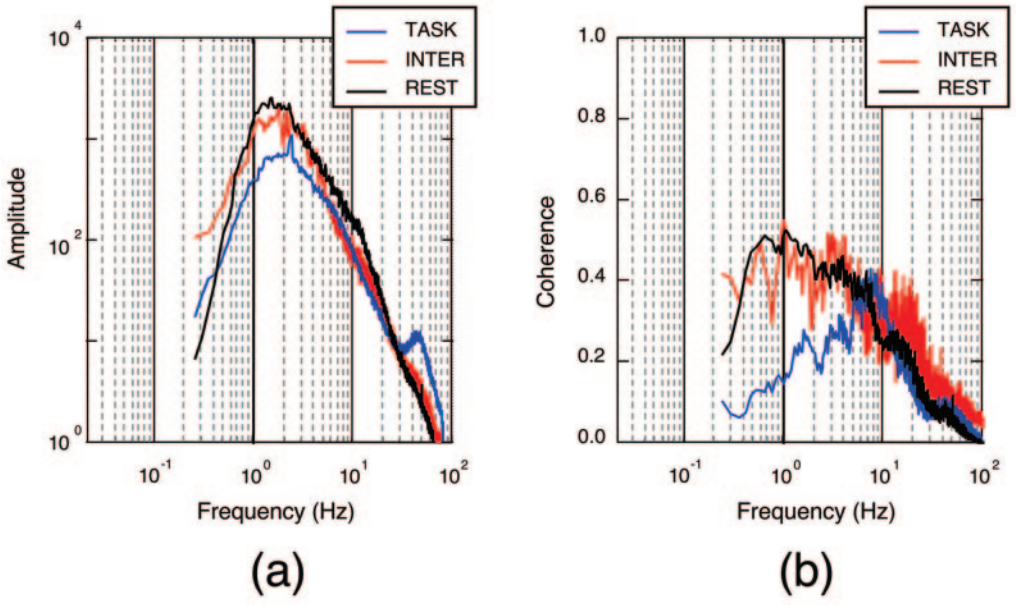

Figure 2. Grand mean power spectrum and coherence of the raw LFP signal during an entire session. The electrode positions and receptive fields for 15 electrodes in the post-lunate visual areas are as depicted in Figure 1*b*. For the data shown here, the monkey was awake and seated, but not engaged in any particular task. His scanning movements around the dim recording room determined the structure of his visual input. (*a*) Power spectral density of the LFP, averaged over all 15 electrodes. (*b*) Mean pairwise cross coherence between all electrode pairs in the array.

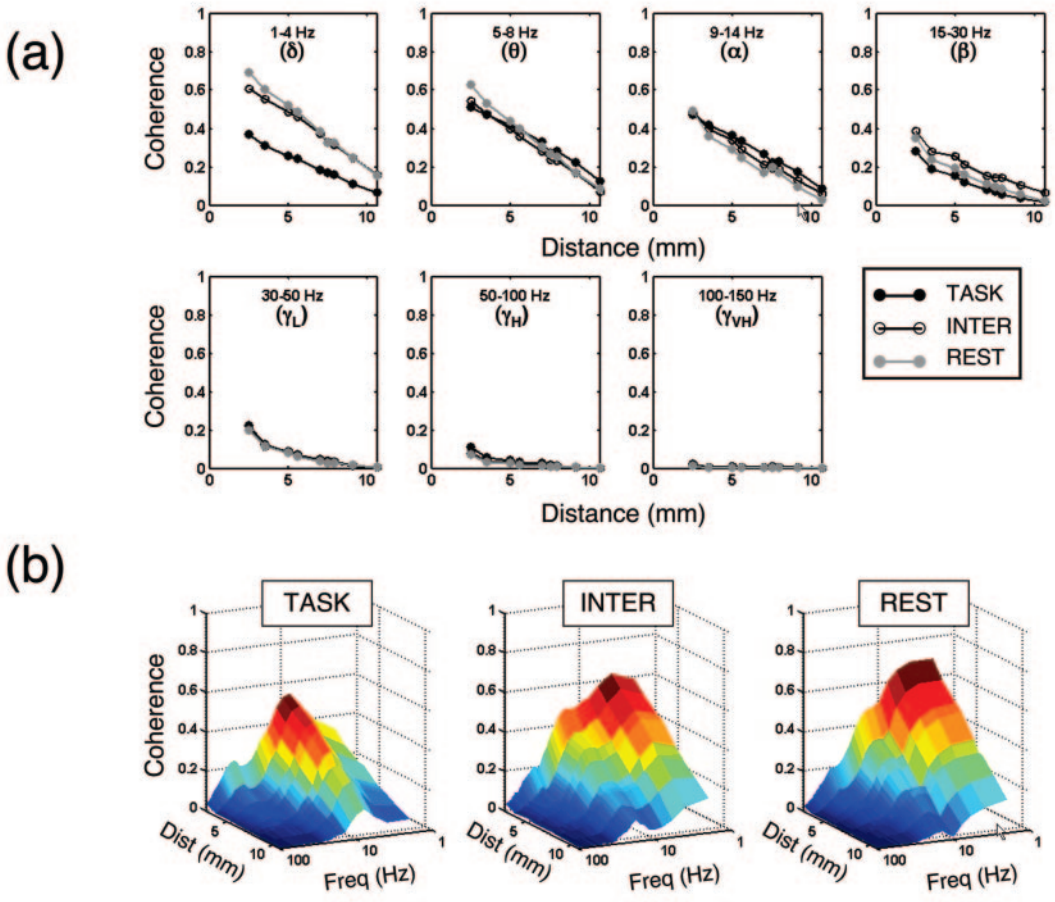

Figure 3. Coherence of raw LFP signal as a function of inter-electrode distance for three behavioral conditions. (*a*) Decline in coherence with increasing electrode separation for each of the three conditions in seven discrete frequency ranges. (●, visual task; ○, inter-trial; ○, resting). (*b*) Three-dimensional representation of LFP coherence as a function of frequency and cortical distance for each condition.

major factor in their coherence, which is in agreement with previous observations (Frien and Eckhorn, 2000). Each plot in Figure 3*a* represents the coherence value in a given frequency range, as a function of inter-electrode distance, for each of the behavioral states in one session. Note that in nearly all cases, coherence values fell to <0.15 for distances >10 mm, even when their values at 2.5 mm were >0.5. In this session, the drop-off was approximately linear for most frequencies. While this was true for some sessions, others displayed significant deviations from linearity. The decline of coherence with distance varied as a function of frequency, as well as behavioral state. For example, during the task, coherence declined more sharply with distance in the 5–8 Hz range than in the 1–4 Hz range. However, this trend was not true in the inter-trial, in which case the decline was similar for the two frequency ranges. Figure 3*b* shows in three dimensions how coherence varied with distance and frequency for each of the behavioral conditions. Note that, in general, coherence fell sharply for both long time-scales (i.e. low frequencies) and large cortical distances.

Coupling of BLP Signals

Given our aim of exploring very slow neural fluctuations, we next evaluated the same data using a method that allowed us to evaluate changes in the local field at arbitrary time-scales. Specifically, we reasoned that although high pass filtering prohibited measurement of slow changes in the raw LFP signal, significant and biologically relevant fluctuations in LFP power might proceed over arbitrarily long time-scales. Furthermore, given the tight coupling between BOLD responses and LFP power (Logothetis *et al.*, 2001), such slow fluctuations would be likely to have a significant impact on signals measured in fMRI. We therefore explored the natural time course of power signals in the visual cortex derived from different frequency ranges of the LFP. We evaluated two aspects of BLP signals (see Materials and Methods and Fig. 4) that are relevant for comparison with functional imaging data. First, we computed the power spectrum of the BLP for each frequency range during the rest condition (Fig. 5*a*). As one might predict from the raw spectra shown in Figure 2*a*, power in the lowest frequency bands (e.g. 1–4 Hz) was higher than that in upper frequency bands (e.g. 100–150 Hz). However, it is interesting to note that very slow BLP fluctuations, displaying changes on the order of tens of s (i.e. <0.1 Hz), had comparatively higher amplitude than the faster BLP fluctuations, proceeding as roughly as $1/f$ for frequencies <2 Hz.

Secondly, we evaluated the mean coherence in the BLP, which is shown in Figure 5*b*, averaged over all electrode pairs. This plot reveals several interesting features about coherence between BLP signals. For example, the coherence values are generally quite large, revealing that a portion of the BLP changes is shared between cortical sites. Also, there is a roughly monotonic trend toward higher coherence at low frequencies, demonstrating that slow changes contribute the most to the inter-electrode covariation. Finally, the frequency ranges displaying the largest coherence at long time-scales were the γ-range frequencies between 30 and 100 Hz. This observation was common in both the rest and task conditions.

The nature of BLP covariation is perhaps best observed in the time domain over periods of several minutes, as shown in Figure 6. In this figure, the δ and γ_L BLP signals for all electrodes

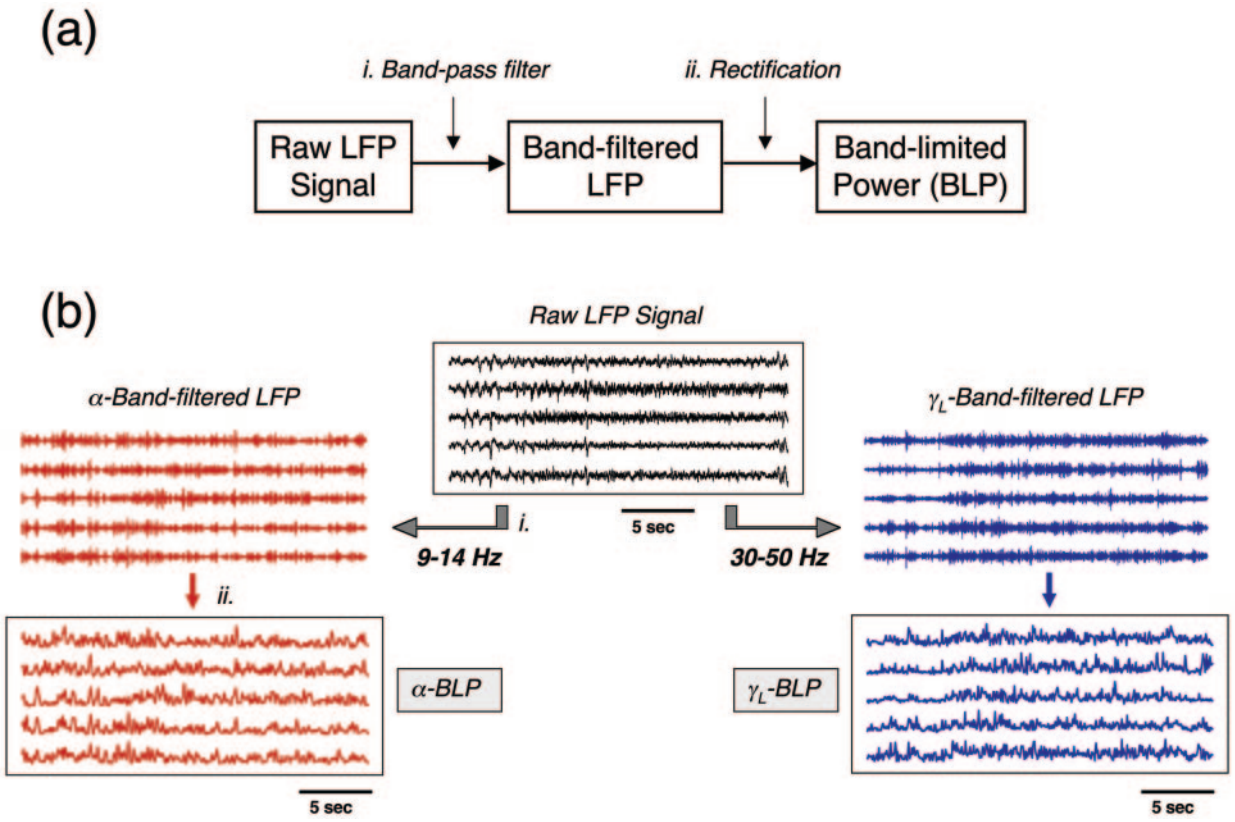

Figure 4. Dissection of raw LFP signal into continuous BLP signals. (*a*) Schematic outlining the general method creating BLP signals. Raw LFP data was first band-pass filtered (i) and then rectified (ii). The resulting signal was then low pass filtered and resampled (not depicted). See Materials and Methods section for details. This procedure was applied to each LFP signal for seven different frequency ranges applied in step (i). (*b*) Example application of this scheme to five simultaneously recorded LFP signals, for two different frequency bands.

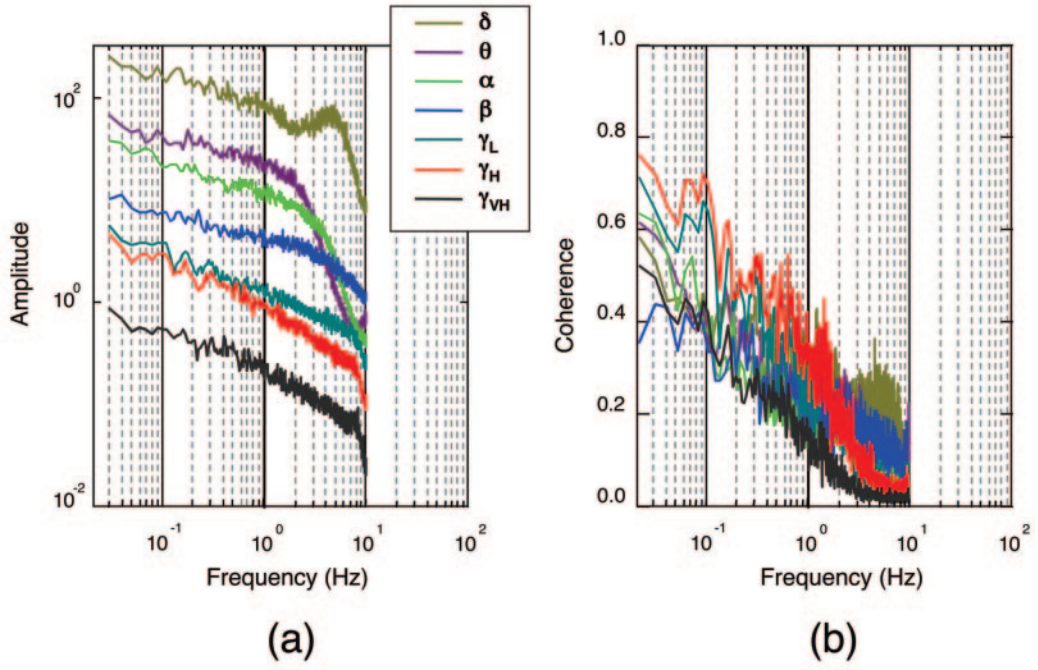

Figure 5. Grand mean power spectrum and coherence of power (rectified) LFP signals during resting condition. (*a*) The power spectrum reveals increased power at lower frequencies resulting from the rectification process. (*b*) As suggested by the example in Figure 5, the coherence between electrodes at long time-scales is also very high for the power signal. Thus, the LFP power displays slow, coordinated changes at long time-scales.

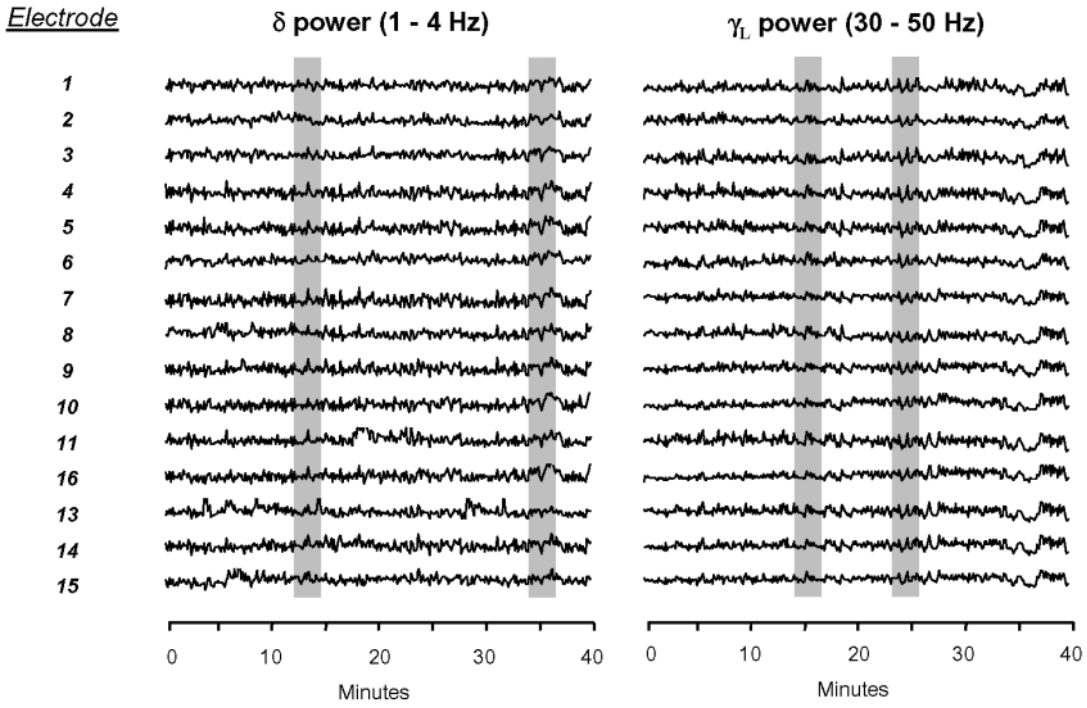

Figure 6. Band-limited power signals across many electrodes over long time-scales. Two examples, representing δ- and γ-band ranges, are shown. Gray shaded areas represent epochs of strong synchronization between all electrodes. The electrode configuration is that shown in Figure 1*b*. Note that in the δ-range and particularly in the γ-range, there is a strong temporal covariation between channels, even at time-scales over many seconds and minutes.

are shown over a period of 40 min with the monkey in the rest state. Inspection revealed many common motifs aligned in time between the different channels (gray shaded regions). This was particularly true in the case of the γ_L power, where some fluctuations were present in all channels, despite electrode separation >10 mm. In accordance with the coherence plots in Figure 5*b*, these shared fluctuations were particularly pronounced for very low frequency changes (<0.1 Hz).

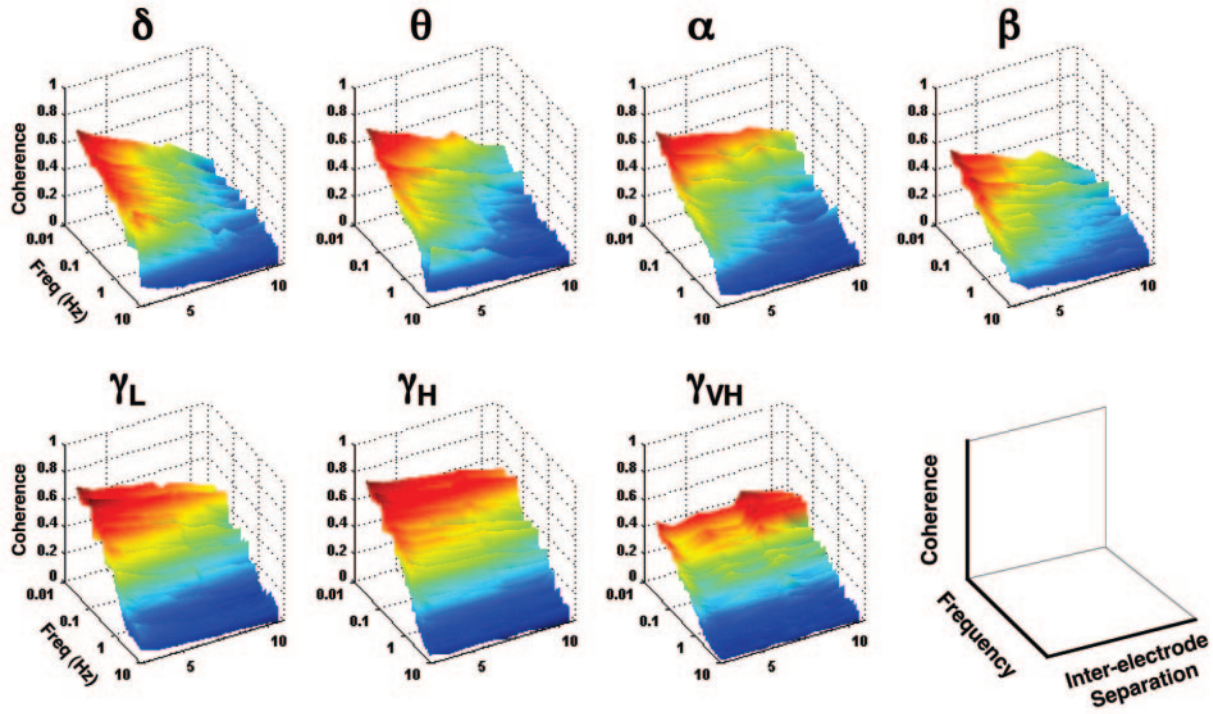

Figure 7. Coherence of BLP signals as a function of frequency and cortical distance during rest condition. Each panel is derived BLP corresponding to a particular frequency band indicated. Coherence is shown as a function of the distance between electrodes (between 2.5 and 10.6 mm), as well as the frequency (between 0.01 and 10 Hz).

Spatial Properties of BLP Coupling

We next investigated how coherence of the BLP depended on inter-electrode separation. Figure 7 illustrates the coherence as a function of frequency and inter-electrode distance for each of the BLP ranges in the rest condition. Note that in each of the plots, the coherence values are particularly high for the lowest frequencies and that this coupling is present over long cortical distances. This is particularly true for BLP signals derived from the γ-range. Figures 8 and 9 compare the coherence-distance relationships for LFP and BLP signals during the rest and task conditions, respectively. For comparison, data from Figure 3*a* is replotted for all frequency bands in Figures 8*a* and 9*a*. In Figures 8*b* and 9*b*, the coherence–distance relationship is shown for the BLP for the same sessions at two time-scales. Each of the colored lines within each panel corresponds to the BLP calculated from a particular frequency band. Note that for the very slow BLP signals, the coherence remains high with increasing inter-electrode distance. This is particularly true for the low and high γ-range power fluctuations (red and cyan curves), which display very high coherence even at separations of >10 mm. The similar appearance of the BLP coherence plots in Figures 8*b* and 9*b* suggest that the basic observation is due neither to the engagement in a task, nor to hypersynchronous cortical activity patterns that might be related to sleep.

Finally, Figure 10 illustrates that strong temporal covariation exists between BLP signals over great cortical distances. Data is shown from a session in which the square electrode array was placed such that a subset of electrodes fell on either side of the lunate sulcus (bottom right). The effective cortical distance between electrodes lying on opposite sides of the sulcus exceeded 25 mm. BLP traces from five frequency bands are shown for prelunate (red) and postlunate (green) electrodes. Note the high correspondence between temporal features in the traces. While there is clearly more similarity between waveforms on the same side of the sulcus, electrodes on opposite sides clearly share a great deal of temporal structure, particularly for BLP signals derived from the higher frequencies.

Discussion

Neural dynamics related to cognition and behavior are generally rapid, proceeding at a rate of milliseconds to seconds. In fMRI, the evaluation of such dynamics remains limited despite the development of techniques to optimize temporal information (Rosen *et al.*, 1998). While the BOLD signal can clearly register the occurrence of brief, singular neural events, it cannot consistently track fast activity changes. For example, recent results demonstrated that neural signals could not be accurately reconstructed from the BOLD signal when changes were faster than ~0.21 Hz (Logothetis, 2002). In the present study, we considered this limitation, and posed the following question: might neural dynamics also express themselves at much slower time-scales that are more compatible with fMRI measurements? We report here that very slow, coherent activity fluctuations do indeed encompass the visual cortex. We believe that these results indicate that large-scale networks in the brain contribute significantly to neural variability observed at a cortical site and furthermore suggest that fMRI may be an excellent tool to monitor and visualize neural activity in such networks.

Global Coherence

The BLP signals, which were derived from the local field, displayed maximal amplitude at very low frequencies. These slow changes were largely shared between electrodes, even for the largest cortical distances tested. This global coherence may provide insight into the nature of the fluctuations themselves, as it is suggestive of interplay with subcortical structures that can

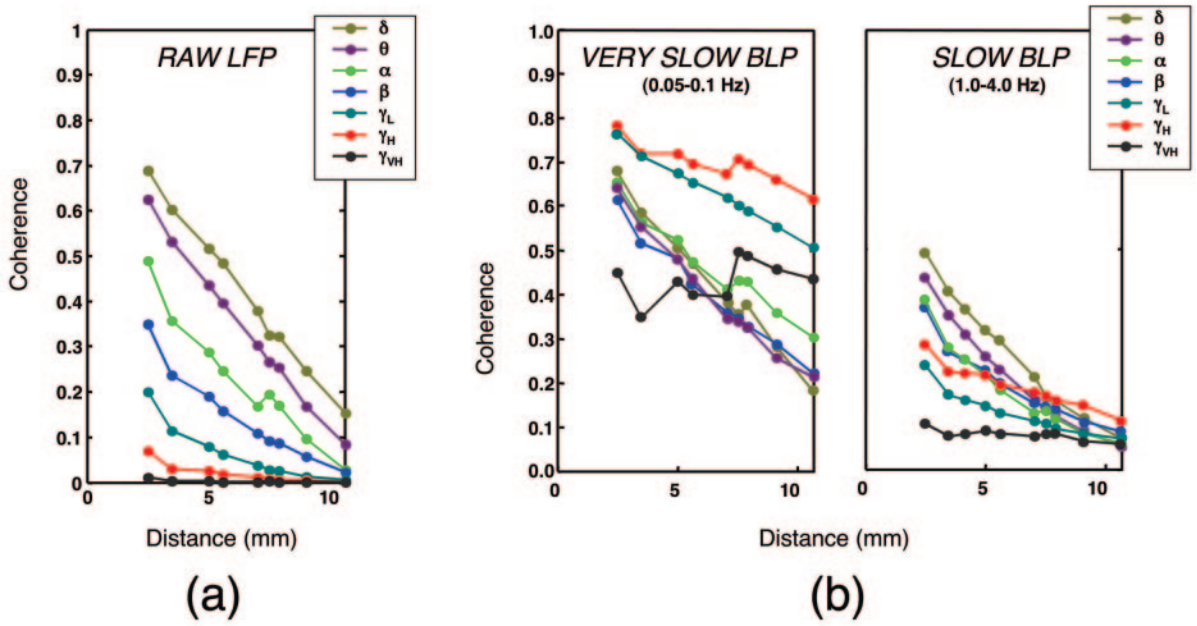

Figure 8. Comparison of coherence drop-off with inter-electrode distance between raw (*a*) and rectified (*b*) LFP signals during the *rest* condition. (*a*) Raw LFP data replotted from Figure 3*a* for each frequency range. (*b*) For each frequency band, the corresponding coherence of the rectified signals is shown for two time-scales. Each color represents a particular pass band, the inter-electrode coherence of which is shown as a function of distance. This method allows one, for example, to estimate the degree of covarying fluctuations of power within a given frequency band over long time-scales. Note that, in contrast to the raw data shown in (*a*), the very slow BLP data in left half of (*b*) does not fall off quickly as a function of cortical distance. This is particularly true for the low and mid γ-range activity.

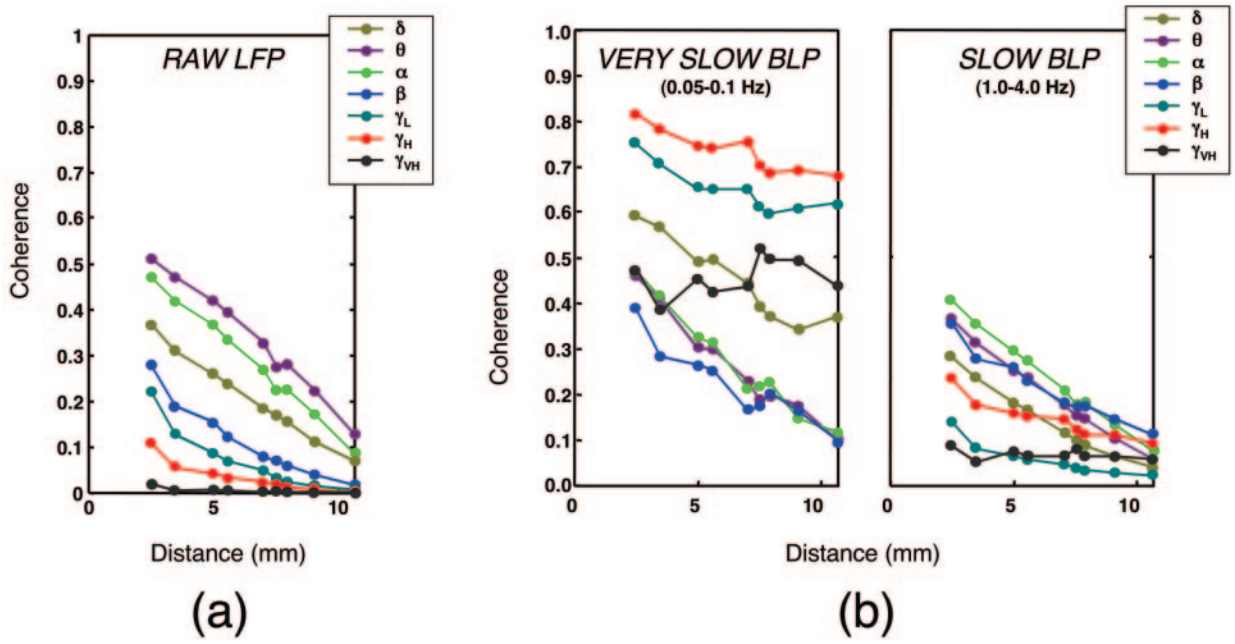

Figure 9. Same format as Figure 8, but during task condition. Data are collected with the same electrodes in the same position. Note that the far-reaching coherence of the BLP, particularly in the γ-range, is fundamentally similar to the rest condition.

simultaneously influence activity across distant cortical sites. It is interesting to note that the frequency bands whose BLP signals showed the highest temporal coherence were in the γ-range. This finding is in some respects counterintuitive, since global synchronization in the brain is often associated with lower frequencies, such as slow cortical rhythms, alpha waves, and sleep spindles (Berger, 1929; Amzica and Steriade, 1995; Contreras *et al.*, 1997; Steriade, 2000). In contrast, γ-range coupling is thought to be more representative of local processing, as observed for the raw LFP coherence in the present study, as well as in several other studies (Steriade *et al.*, 1996a, b; Frien and Eckhorn, 2000), but see Murthy and Fetz (Murthy and Fetz, 1996). While one might therefore predict that γ-derived BLP fluctuations would also fall off quickly with distance, we

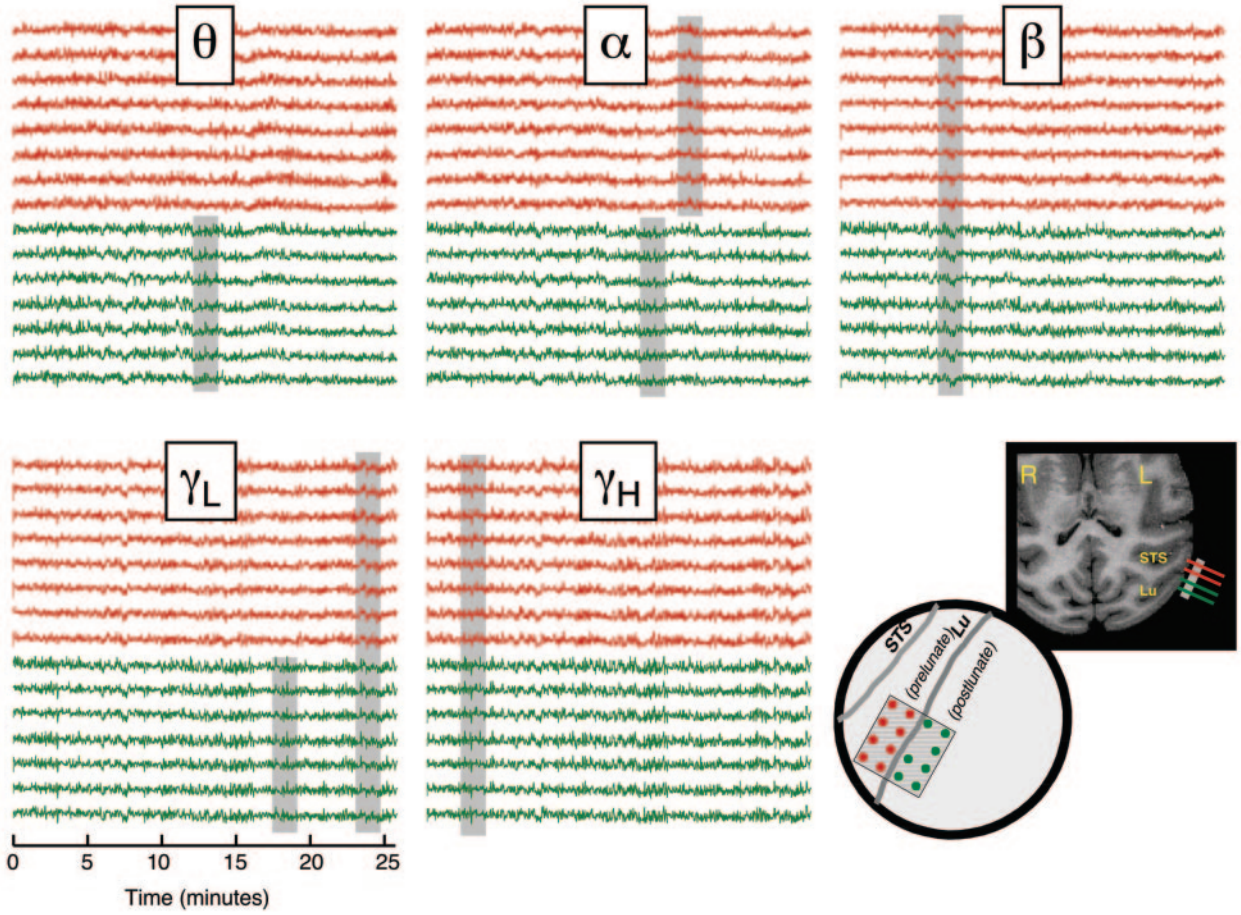

Figure 10. BLP signals from 15 electrodes distributed on opposite sides of the lunate sulcus. With this position, the effective cortical separation of the prelunate (red) and postlunate (green) sites was much larger than their physical separation (see depiction of electrodes in chamber and on MRI image in lower right). Each panel shows the BLP from all 15 electrodes derived from a particular frequency range. Gray shaded areas highlight periods of close temporal agreement in the slow fluctuations, in some cases restricted to within an area and in others shared between all electrodes.

report here that it is, in contrast, the most coherent of all frequency bands, with only minimal decrease in coherence over cortical distances exceeding 10 mm. Note that the coherence described here is not cycle-to-cycle coherence in the γ voltage, but rather slow, shared fluctuations in the γ power. Interestingly, a fundamentally similar technique was previously applied in a study involving human subdural recordings (Bruns *et al.*, 2000). In that study, the authors evaluated coherent fluctuations in the amplitude envelope of the filtered γ-range activity (equivalent to the γ-BLP) and similarly found that coupling could be detected in the modulation of this 'carrier' signal when it was absent in the raw signals.

The far-reaching spatial coherence of power fluctuations, contrasted with the highly localized coherence of the raw voltage signals, raises the interesting possibility that these two aspects of neural dynamics represent different dimensions of cortical, and perhaps thalamocortical, processing. Much evidence has supported the idea that coupling of the local sensory circuitry, particularly in the γ range, may important for the pattern encoding, and perhaps for aspects of higher perceptual processing (Singer and Gray, 1995; Eckhorn, 2000; Gail *et al.*, 2000; Fries *et al.*, 2001). In contrast, the slow, coherent power fluctuations we report here are widespread and are therefore unlikely to be involved in highly specific pattern analysis. Instead, these fluctuations might represent a more global, coordinative aspect of thalamocortical processing, where the strength or efficacy of localized processing at distant brain regions can be modulated, without disrupting specific coupling mechanisms within a region. Further experiments are needed to determine whether these slow power modulations are restricted to the visual cortex, or if they also impact other sensory and non-sensory cortical areas.

Possible Consequences and Origins of Slow Fluctuations

It is interesting to note that despite the brain's remarkable capacity to contend with its own variability, there may indeed be behavioral consequences of the slow fluctuations of the type reported here. Evidence for this possibility comes from a comparison of our results with human behavioral studies. When humans perform a cognitive task repetitively over extended periods of time, their task performance is not stationary, but instead tends to fluctuate over periods of s and min. Careful analysis of this temporal instability revealed that the changes have a '1/*f* noise' quality (Gilden *et al.*, 1995; Gilden, 2001). It is intriguing to speculate that such fluctuations arise from endogenous activity changes that influence cognitive processing. It is therefore notable that the BLP spectra reported in the present study (Fig. 5*a*) bear a striking resemblance to those derived from human performance fluctuations, for example as shown in Figure 1*a* of Gilden *et al.* (Gilden *et al.*, 1995). It is

possible that spontaneous activity changes in the cortex over long time-scales contribute significantly to the fine-tuning of our perceptual and behavioral capabilities.

Additional evidence linking our results with behavioral studies arises from several electrophysiological studies that correlate performance with activity in the brainstem. For example, activity in the locus coeruleus was shown to co-fluctuate with behavioral performance of monkeys in a visual discrimination task over long time-scales (Aston-Jones *et al.*, 1994; Usher *et al.*, 1999). Noradrenergic neurons in this structure project diffusely throughout the cortex and are thought to play a modulatory role in nonspecific aspects of behavior, such as motivation and arousal (Foote and Morrison, 1987; Berridge and Foote, 1991). Similarly, the role of the midbrain reticular formation (MRF) in cortical activation and arousal has long been recognized (Moruzzi and Magoun, 1949). Early studies revealed that electrical stimulation of the MRF enhanced the processing of sensory stimuli (Dumont and Dell, 1960) and could actually improve tachistoscopic performance in a monkey performing a discrimination task (Fuster, 1957). More recently, functional imaging in humans revealed that this area was specifically activated during tasks that required a high attentional demand (Kinomura *et al.*, 1996). Together, these studies suggest that the slow fluctuations we observe may be under brainstem control, and may be related to behavioral fluctuations. The predominance of synchronization of γ-range BLP signals may also be of particular interest given the postulated role of γ-range activity and synchronization in cortical activation (Moruzzi and Magoun, 1949; Munk *et al.*, 1996), sensory processing (Eckhorn *et al.*, 1988; Singer and Gray, 1995), attention (Fries *et al.*, 2001) and perhaps even conscious perception (Llinas and Ribary, 1993, Engel *et al.*, 1999).

However, it is important to note that in the present study the slow, coherent fluctuations in the BLP signals were not unique to the task condition, but were equally pronounced during the rest conditions, where the animal's external behavior was very different. Preliminary results also indicate that BLP signals, including pronounced coherence of the γ-derived signals, are similar in monkeys under light general anesthesia (D.A. Leopold, unpublished observations). Thus, while the very slow, coherent fluctuations we report may be related to active elements of attention and perception, they also appear to be present in states of diminished consciousness, suggesting that their generation is not specific to a particular cognitive or behavioral context.

In order to understand better the nature of these changes, it might be informative to learn how they relate to other aspects of brain physiology. For example, recent work from Raichle and colleagues in human fMRI and positron emission tomography (PET) has also emphasized the need to examine activity in the absence of a stimulus or a task in order to correctly interpret an evoked response (Gusnard and Raichle, 2001). These experiments have not examined neural activity directly, but have used measures of hemodynamic and metabolic signals acquired through imaging to attempt to establish a general notion of 'activation' for brain tissue. One computed variable, the oxygen extraction fraction (the ratio of oxygen utilized in a portion of tissue to that delivered) can, under conditions of rest, show remarkable spatial uniformity across the entire brain despite large local differences in the measured variables used to compute it. This finding led Raichle to suggest that the very notion of an 'activity baseline' in the brain need not be an arbitrary experimental reference point, but might instead reflect a well-defined physiological state of brain tissue. How then might the slow, spontaneous electrical fluctuations reported here relate to such a baseline? While it is still too early to answer this question, preliminary data from our laboratory suggest that the baseline activity might be significantly affected by the BLP fluctuations reported here (Leopold *et al.*, 2002). We simultaneously measured LFP from one electrode in the visual cortex and fMRI signals over the entire brain in the anesthetized monkey whose eyes were closed. We found that the time course of the BOLD signal was often highly correlated with the spontaneous neural activity (BLP) fluctuations. Moreover, although the electrical signal came from a single electrode, the correlations often reached over large stretches of the cerebral cortex — in some cases nearly the entire brain. Given that the BOLD changes are correlated with those of the oxygen extraction fraction, this finding might suggest that even the spatially uniform 'default state' relevant for imaging studies is subject to spontaneous fluctuations resulting from underlying slow changes in neural activity. We are currently investigating the degree to which these slow fluctuations impact the firing rate of individual neurons. It would be, for example, particularly interesting if one type or layer of cortical neurons consistently modulated with global baseline fluctuations, while another did not.

A Neural Reference for Functional Imaging Studies

Given the comparable time courses of the BLP and BOLD signals, as well as the preliminary results mentioned above, there are at least two reasons why combined electrophysiological and fMRI techniques may be of great value in exploring brain function. First, combined measurements might be performed to explore functional connectivity of global networks that are otherwise inaccessible. Traditionally, the use of fMRI to assess functional interactions in the brain has exploited covariation in the time course of voxels in distant brain regions, since even in the resting brain voxel intensity varies on the order of 1–2% (Biswal *et al.*, 1997). Such covariation analysis has been applied in studies with subjects at rest (Biswal *et al.*, 1997; Lowe *et al.*, 1998; Xiong *et al.*, 1999; Cordes *et al.*, 2001), or engaged in a motor or cognitive task (Lumer and Rees, 1999; Cordes *et al.*, 2000). Unfortunately, coherent temporal fluctuations can arise from a diversity of sources that are not directly linked to underlying neural activity. Such sources include periodic cardiac and respiratory noise (Frank *et al.*, 2001; Lund, 2001), slow, autonomous hemodynamic regulation (Obrig *et al.*, 2000) and magnetic field drift (Durand *et al.*, 2001). While several methods have been developed to identify and remove artifacts caused by the periodic physiological signals (Glover *et al.*, 2000; Chuang and Chen, 2001) these methods often rely upon high image acquisition rates in order to meet the Nyquist criterion for temporal sampling. High-speed scanning usually comes at the expense of spatial coverage and image quality, which are both particularly important for investigating functional interactions between distant brain areas. Other strategies for removing such artifacts include the use of blind source separation techniques (McKeown *et al.*, 1998; Arfanakis *et al.*, 2000).

The simultaneous monitoring of BOLD and LFP signals may significantly refine one's ability to focus on temporal covariation that is related to underlying changes in neural activity. By using the BLP signal as a reference signal it may be possible to focus on BOLD fluctuations that are specifically tied to neural changes. Previous approaches using combined electrical and fast optical-imaging techniques have allowed for remarkable visualization of localized cortical networks (Arieli *et al.*, 1996; Tsodyks *et al.*, 1999; Seidemann *et al.*, 2002). Given the spatial coverage of fMRI, it would be of great value to use a signal such as the BLP to

isolate and visualize global brain networks that contribute to its fluctuations. Interestingly, its profound coherence between distant electrodes suggests that a single cortical electrode could serve as a reference for very large cortical region, perhaps even for the entire brain. As mentioned above, preliminary experiments from our laboratory suggest that this is indeed the case. Thus, monitoring the signal of a single electrode during imaging might facilitate the visualization of global brain networks that could not otherwise be tapped.

The second reason to combine these techniques centers on the potential contribution of the slow BLP modulations reported here to the 1–2% physiological fluctuations in the BOLD signal. As argued above, these changes may be of great important to understanding brain function, and may even underlie dynamic aspects of our perception and cognition. However, in many fMRI paradigms, such slow changes are unrelated to the presentation of a stimulus or the execution of a task and might therefore be a considered a source of neural 'pollution' for a particular experiment. In such cases, it might be of great value to measure and remove fluctuations in the signal related to these slow neural changes, a manipulation that might greatly improve the signal-to-noise ratio within an fMRI experiment and thereby reduce the required number of averages. In the experimental animal, this might take the form of an implanted intracortical electrode, through which the LFP is monitored during functional imaging. In humans, it is possible that a single EEG reference might be able to provide a similar function. Additional experiments are needed to determined whether the combined monitoring of electrical and fMRI signals will lead to significant improvement in the visualization of brain function, either in the context of mapping networks involved in generating spontaneous changes as reported here, or for eliminating unwanted neural contributions in a traditional fixed fMRI paradigm.

Notes

The authors would like to thank Dr A.A. Ghazanfar, A. Maier and M. Wilke for comments on an earlier version of the manuscript, Drs J. Pfeuffer and P. Mitra, and A. Oeltermann for discussion, and Dr W. S. Geisler for pointing out the connection with performance fluctuations in human psychophysics. In addition, we thank C. Moya and J. Werner for technical assistance. This work was supported by the Max Planck Society.

Address correspondence to David A. Leopold, Max Planck Institut für biologische Kybernetik, Spemannstraße 38, 72076 Tübingen, Germany. Email: david.leopold@tuebingen.mpg.de.

References

Amzica F, Steriade M (1995) Short- and long-range neuronal synchronization of the slow (<1 Hz) cortical oscillation. J Neurophysiol 73:20–38.

Arfanakis K, Cordes D, Haughton VM, Moritz CH, Quigley MA, Meyerand ME (2000) Combining independent component analysis and correlation analysis to probe interregional connectivity in fMRI task activation datasets. Magn Reson Imaging 18:921–930.

Arieli A, Shoham D, Hildesheim R, Grinvald A (1995) Coherent spatiotemporal patterns of ongoing activity revealed by real-time optical imaging coupled with single-unit recording in the cat visual cortex. J Neurophysiol 73:2072–2093.

Arieli A, Sterkin A, Grinvald A, Aertsen A (1996) Dynamics of ongoing activity: explanation of the large variability in evoked cortical responses. Science 273:1868–1871.

Aston-Jones G, Rajkowski J, Kubiak P, Alexinsky T (1994) Locus coeruleus neurons in monkey are selectively activated by attended cues in a vigilance task. J Neurosci 14:4467–4480.

Azouz R, Gray CM (1999) Cellular mechanisms contributing to response variability of cortical neurons *in vivo*. J Neurosci 19:2209–2223.

Bauer HH, Rebert CS (1990) Preliminary study on subcortical slow potentials related to the readiness potential in the monkey. Int J Psychophysiol 9:269–278.

Berger H (1929) Ueber das Elektroencephalogramm des Menchen. Arch Psychiatrie Nervenkrankh 87:527–570.

Berridge CW, Foote SL (1991) Effects of locus coeruleus activation on electroencephalographic activity in neocortex and hippocampus. J Neurosci 11:3135 –3145.

Biswal BB, Van K, Hyde JS (1997) Simultaneous assessment of flow and BOLD signals in resting-state functional connectivity maps. NMR Biomed 10:165–170.

Bonmassar G, Schwartz DP, Liu AK, Kwong KK, Dale AM, Belliveau JW (2001) Spatiotemporal brain imaging of visual-evoked activity using interleaved EEG and fMRI recordings. Neuroimage 13:1035–1043.

Bruns A, Eckhorn R, Jokeit H, Ebner A (2000) Amplitude envelope correlation detects coupling among incoherent brain signals. Neuroreport 11:1509–1514.

Bullier J, Nowak LG (1995) Parallel versus serial processing: new vistas on the distributed organization of the visual system. Curr Opin Neurobiol 5:497–503.

Chuang KH, Chen JH (2001) IMPACT: image-based physiological artifacts estimation and correction technique for functional MRI. Magn Reson Med 46:344–353.

Contreras D, Destexhe A, Sejnowski TJ, Steriade M (1997) Spatiotemporal patterns of spindle oscillations in cortex and thalamus. J Neurosci 17:1179–1196.

Cordes D, Haughton VM, Arfanakis K, Wendt GJ, Turski PA, Moritz CH, Quigley MA, Meyerand ME (2000) Mapping functionally related regions of brain with functional connectivity MR imaging. Am J Neuroradiol 21:1636–1644.

Cordes D, Haughton VM, Arfanakis K, Carew JD, Turski PA, Moritz CH, Quigley MA, Meyerand ME (2001) Frequencies contributing to functional connectivity in the cerebral cortex in 'resting-state' data. AJNR Am J Neuroradiol 22:1326–1333.

Dumont S, Dell P (1960) Facilitation reticulaire des mecanismes visuels corticaux. Electroencephalogr Clin Neurophysiol 12:769–796.

Durand E, Van D, Pachot-Clouard M, Le B (2001) Artifact due to B(0) fluctuations in fMRI: correction using the k-space central line. Magn Reson Med 46:198–201.

Eckhorn R (2000) Cortical synchronization suggests neural principles of visual feature grouping. Acta Neurobiol Exp 60:261–269.

Eckhorn R, Thomas U (1993) A new method for the insertion of multiple microprobes into neural and muscular tissue, including fiber electrodes, fine wires, needles and microsensors. J Neurosci Methods 49:175–179.

Eckhorn R, Bauer R, Jordan W, Brosch M, Kruse W, Munk M, Reitboeck HJ (1988) Coherent oscillations: a mechanism of feature linking in the visual cortex? Multiple electrode and correlation analyses in the cat. Biol Cybern 60:121–130.

Engel AK, Fries P, Konig P, Brecht M, Singer W (1999) Temporal binding, binocular rivalry, and consciousness. Conscious Cogn 8:128–151.

Foote SL, Morrison JH (1987) Extrathalamic modulation of cortical function. Annu Rev Neurosci 10:67–95.

Frackowiak RS, Friston KJ, Frith CD, Dolan RJ, Mazziotta JC (1997) Human brain function, vol. 1. San Diego, CA: Academic Press.

Frank LR, Buxton RB, Wong EC (2001) Estimation of respiration-induced noise fluctuations from undersampled multislice fMRI data. Magn Reson Med 45:635–644.

Frien A, Eckhorn R (2000) Functional coupling shows stronger stimulus dependency for fast oscillations than for low-frequency components in striate cortex of awake monkey. Eur J Neurosci 12:1466–1478.

Fries P, Reynolds JH, Rorie AE, Desimone R (2001) Modulation of oscillatory neuronal synchronization by selective visual attention. Science 291:1560–1563.

Fuster JM (1957) Tachistoscopic perception in monkeys. Fed Proc 16:43.

Gail A, Brinksmeyer HJ, Eckhorn R (2000) Contour decouples gamma activity across texture representation in monkey striate cortex. Cereb Cortex 10:840–850.

Gilden DL (2001) Cognitive emissions of 1/*f* noise. Psychol Rev 108:33–56.

Gilden DL, Thornton T, Mallon MW (1995) 1/*f* noise in human cognition. Science 267:1837–1839.

Glover GH, Li TQ, Ress D (2000) Image-based method for retrospective correction of physiological motion effects in fMRI: RETROICOR. Magn Reson Med 44:162–167.

Gusnard DA, Raichle ME (2001) Searching for a baseline: functional imaging and the resting human brain. Nat Rev Neurosci 2:685–694.

Heinze HJ, Mangun GR, Burchert W, Hinrichs H, Scholz M, Munte TF,

Gos A, Scherg M, Johannes S, Hundeshagen H (1994) Combined spatial and temporal imaging of brain activity during visual selective attention in humans. Nature 372:543–546.
Hupe JM, James AC, Payne BR, Lomber SG, Girard P, Bullier J (1998) Cortical feedback improves discrimination between figure and background by V1, V2 and V3 neurons. Nature 394:784–787.
Kara P, Reinagel P, Reid RC (2000) Low response variability in simultaneously recorded retinal, thalamic, and cortical neurons. Neuron 27:635–646.
Kinomura S, Larsson J, Gulyas B, Roland PE (1996) Activation by attention of the human reticular formation and thalamic intralaminar nuclei. Science 271:512–515.
Lamme VA, Roelfsema PR (2000) The distinct modes of vision offered by feedforward and recurrent processing. Trends Neurosci 23:571–579.
Lamme VA, Super H, Spekreijse H (1998) Feedforward, horizontal, and feedback processing in the visual cortex. Curr Opin Neurobiol 8:529–535.
Leopold DA, Logothetis NK (1996) Activity changes in early visual cortex reflect monkeys' percepts during binocular rivalry. Nature 379:549–553.
Leopold DA, Augath MA, Logothetis NK (2001) Visualizing global brain networks in the monkey using combined fMRI and electrophysiology. Soc Neurosci Abstr 325:7.
Leopold DA, Plettenberg HK, Logothetis NK (2002) Visual processing in the ketamine-anesthetized monkey: optokinetic and blood oxygenation level-dependent responses. Exp Brain Res 143:359–372.
Llinas R, Ribary U (1993) Coherent 40-Hz oscillation characterizes dream state in humans. Proc Natl Acad Sci USA 90:2078–2081.
Logothetis NK (2002) On the neural basis of the blood oxygen level dependent function magnetic resonance imaging signal. Phil Trans Royal Soc Biol Sci 357:1003–1037.
Logothetis NK, Guggenberger H, Peled S, Pauls J (1999) Functional imaging of the monkey brain. Nat Neurosci 2:555–562.
Logothetis NK, Pauls J, Augath M, Trinath T, Oeltermann A (2001) Neurophysiological investigation of the basis of the fMRI signal. Nature 412:150–157.
Lowe MJ, Mock BJ, Sorenson JA (1998) Functional connectivity in single and multislice echoplanar imaging using resting-state fluctuations. Neuroimage 7:119–132.
Lumer ED, Rees G (1999) Covariation of activity in visual and prefrontal cortex associated with subjective visual perception. Proc Natl Acad Sci USA 96:1669–1673.
Lund TE (2001) fcMRI — mapping functional connectivity or correlating cardiac-induced noise. Magn Reson Med 46:628–629.
McKeown MJ, Makeig S, Brown GG, Jung TP, Kindermann SS, Bell AJ, Sejnowski TJ (1998) Analysis of fMRI data by blind separation into independent spatial components. Hum Brain Mapp 6:160–188.
Moruzzi G, Magoun HW (1949) Brain stem reticular formation and activation of the EEG. Electroencephalogr Clin Neurophysiol 1:455–473.
Munk MH, Roelfsema PR, Konig P, Engel AK, Singer W (1996) Role of reticular activation in the modulation of intracortical synchronization. Science 272:271–274.
Murthy VN, Fetz EE (1996) Oscillatory activity in sensorimotor cortex of awake monkeys: synchronization of local field potentials and relation to behavior. J Neurophysiol 76:3949–3967.
Nicolelis MA, Baccala LA, Lin RC, Chapin JK (1995) Sensorimotor encoding by synchronous neural ensemble activity at multiple levels of the somatosensory system. Science 268:1353–1358.
Obrig H, Neufang M, Wenzel R, Kohl M, Steinbrink J, Einhaupl K, Villringer A (2000) Spontaneous low frequency oscillations of cerebral hemodynamics and metabolism in human adults. Neuroimage 12:623–639.
Ogawa S, Lee TM, Stepnoski R, Chen W, Zhu XH, Ugurbil K (2000) An approach to probe some neural systems interaction by functional MRI at neural time scale down to milliseconds. Proc Natl Acad Sci USA 97:11026–11031.
Ramcharan EJ, Gnadt JW, Sherman SM (2000) Burst and tonic firing in thalamic cells of unanesthetized, behaving monkeys. Vis Neurosci 17:55–62.
Rosen BR, Buckner RL, Dale AM (1998) Event-related functional MRI: past, present, and future. Proc Natl Acad Sci USA 95:773–780.
Schmolesky MT, Wang Y, Hanes DP, Thompson KG, Leutgeb S, Schall JD, Leventhal AG (1998) Signal timing across the macaque visual system. J Neurophysiol 79:3272–3278.
Schroeder CE, Mehta AD, Givre SJ (1998) A spatiotemporal profile of visual system activation revealed by current source density analysis in the awake macaque. Cereb Cortex 8:575–592.
Seidemann E, Arieli A, Grinvald A, Slovin H (2002) Dynamics of depolarization and hyperpolarization in the frontal cortex and saccade goal. Science 295:862–865.
Sherman SM, Guillery RW (2000) Exploring the thalamus, vol. 1. San Diego, CA: Academic Press.
Singer W, Gray CM (1995) Visual feature integration and the temporal correlation hypothesis. Annu Rev Neurosci 18:555–586.
Steriade M (2000) Corticothalamic resonance, states of vigilance and mentation. Neuroscience 101:243–276.
Steriade M (2001a) Impact of network activities on neuronal properties in corticothalamic systems. J Neurophysiol 86:1–39.
Steriade M (2001b) To burst, or rather, not to burst. Nat Neurosci 4:671–672.
Steriade M, Amzica F, Contreras D (1996a) Synchronization of fast (30–40 Hz) spontaneous cortical rhythms during brain activation. J Neurosci 16:392–417.
Steriade M, Contreras D, Amzica F, Timofeev I (1996b) Synchronization of fast (30–40 Hz) spontaneous oscillations in intrathalamic and thalamocortical networks. J Neurosci 16:2788–2808.
Tsodyks M, Kenet T, Grinvald A, Arieli A (1999) Linking spontaneous activity of single cortical neurons and the underlying functional architecture. Science 286:1943–1946.
Usher M, Cohen JD, Servan-Schreiber D, Rajkowski J, Aston-Jones G (1999) The role of locus coeruleus in the regulation of cognitive performance. Science 283:549–554.
von Stein A, Chiang C, Konig P (1997) Top-down processing mediated by interareal synchronization. Proc Natl Acad Sci USA 97:14748–14753.
Xiong J, Parsons LM, Gao JH, Fox PT (1999) Interregional connectivity to primary motor cortex revealed using MRI resting state images. Hum Brain Mapp 8:151–156.